Impact of Air Velocity on the Detection of Fires in Conveyor Belt Haulageways

Inoka Eranda Perera and Charles D. Litton, Pittsburgh Research Laboratory, National Institute for Occupational Safety and Health, PO Box 18070, 626 Cochrans Mill Road, Pittsburgh, PA 15236, USA*
e-mail: CLitton@cdc.gov

Abstract. A series of large-scale experiments were conducted in an above-ground fire gallery using three different types of fire-resistant conveyor belts and four air velocities for each belt. The goal of the experiments was to understand and quantify the effects of air velocity on the detection of fires in underground conveyor belt haulageways and to determine the rates of generation of toxic gases and smoke as a fire progresses through the stages of smoldering coal, flaming coal, and finally a flaming conveyor belt. In the experiments, electrical strip heaters, imbedded approximately 5 cm below the top surface of a large mass of coal rubble, were used to ignite the coal, producing an open flame. The flaming coal mass subsequently ignited 1.83-m-wide conveyor belts located approximately 0.30 m above the coal surface. Gas samples were drawn through an averaging probe for continuous measurement of CO, CO_2, and O_2 as the fire progressed. Approximately 20 m from the fire origin and 0.5 m below the roof of the gallery, two commercially available smoke detectors, a light obscuration meter, and a sampling probe for measurement of total mass concentration of smoke particles were placed. Two video cameras were located upstream of the fire origin and along the gallery at about 14 m and 5 m in order to detect both smoke and flames from the fire. This paper discusses the impact of ventilation airflow on alarm times of the smoke detectors and video cameras, CO levels, smoke optical densities and smoke obscuration, total smoke mass concentrations, and fire heat release rates, examining how these various parameters depend upon air velocity and air quantity, the product of air velocity, and entry cross-section.

1. Introduction

Fires in underground mines represent a significant and potentially catastrophic hazard. Early and accurate detection is one of the keys to minimizing this hazard and its possible consequences. Conveyor belt entries are of particular concern for a variety of reasons. First, conveyor belt entries may extend for thousands of feet with only periodic inspections, often at long intervals corresponding to the beginning and ending of shift changes. Because fires can develop rapidly along these entries, the need for some type of automatic fire detection and warning system becomes readily apparent [1–3]. As examples, the Marianna Mine Fire in 1988

* Correspondence should be addressed to: Inoka Eranda Perera, E-mail: EPerera@cdc.gov

and the Aracoma Mine Fire in 2006 both developed rapidly (10 min to 20 min) along a conveyor belt entry with disastrous consequences [4, 5]. Second, some mines need to use the conveyor entry as an intake entry to supply additional fresh air for a working section. Because the toxic combustion products and smoke from a fire travel with the ventilation airflow, the possibility for rapid and significant contamination of a working section greatly increases the hazard potential, thus placing a greater burden on the fire detection and warning system [1]. Third, the conveyor belt represents an essentially continuous source of fuel running the length of an entry, with previous experiments indicating the potential for rapid flame spread along the conveyor belt surfaces [2]. During rapid flame spread, tremendous heat may be generated along with potentially lethal levels of CO and smoke. The resultant large fires also alter an entry's resistance to airflow [3], thus producing dramatic effects on the mine ventilation flow patterns which can, in turn, adversely impact evacuation and control measures.

Fires within conveyor belt entries typically develop in three stages. First, loose coal from the conveyor belt deposits along a conveyor idler or electrical cable. If the idler begins to overheat due to friction or if there is an electrical fault in a cable, the heat generated is dissipated within the loose coal, producing low-temperature smoldering combustion. Secondly, as the coal temperature increases, fuel vapors from the smoldering coal ignite, producing visible flame from the loose coal, which begins to spread across the surfaces of the coal. Thirdly, when the flames from the coal fire impinge upon the surfaces of the conveyor belt for a sufficient period of time, then the surface of the conveyor belt ignites and the flames begin to spread along the conveyor belt surfaces. When the heat release rate from the burning conveyor belt is of sufficient intensity, then rapid flame spread along the surface of the conveyor belt can occur, producing disastrous consequences.

In the early 1990s, a series of large-scale experiments were conducted to simulate this fire scenario, and the data were used to develop a set of guidelines for fire detection systems [1]. A major constraint of these guidelines was that the actual detection and subsequent alarm of the fire detection system must occur just prior to ignition of the conveyor belt. Once the conveyor belt is ignited, the potential for rapid flame spread with large fires producing copious levels of toxic gases and smoke increases dramatically. If detection/alarm is not achieved before belt ignition, the chances for successful evacuation and control of the fire can be significantly diminished. It should be noted that detection can occur anytime before belt ignition (minutes, seconds, or hours), with the criterion fixed so that one second before belt ignition satisfies the criterion just as adequately as 1 h before belt ignition.

Since these guidelines were developed, the regulations put forward by the Mine Safety and Health Administration (MSHA) have changed, omitting the requirement for point-type heat sensors along conveyor belt entries and replacing this with a requirement for CO sensors or their equivalent [6]. In addition to these regulatory changes, recent recommendations were made for the widespread use of smoke sensors for early warning fire detection in conveyor belt haulageways by the Technical Study Panel on the Utilization of Belt Air and the Composition and Fire Retardant Properties of Belt in Underground Coal Mining [7]. Further, there

has been an increase in the use of wider conveyor belts for transport of coal, leading to concern as to whether the use of wider belts and higher belt air ventilation velocities impacts the fire detection guidelines for spacing and alarm levels.

In order to understand the possible impact of wider belts (1.8 m as opposed 1 m belts used before) to on the fire detection process at different ventilation airflows, a series of experiments were conducted by the National Institute for Occupational Safety and Health (NIOSH) in an above-ground Fire Suppression Facility (FSF), located near Pittsburgh, PA. Tests were conducted at air velocities of 1.0 m/s (200 fpm), 2.0 m/s (400 fpm), 4.1 m/s (800 fpm), and 6.9 m/s (1350 fpm), representative of airflows commonly found in underground coal mines. Using the nomographs [1] for the 300 m (1000 ft) sensor spacing, the respective CO alarm levels were found to be 9 ppm at 1.0 m/s, 5 ppm at 2.0 m/s, 3 ppm at 4.1 m/s, and 1 ppm at 6.9 m/s. Similarly, for smoke sensors spaced at 300 m, the required alarm levels were 0.044 m^{-1} at air velocities of 1.0 m/s and 2.0 m/s, and 0.022 m^{-1} at air velocities of 4.1 m/s and 6.9 m/s.

2. Experiments

Figure 1 shows photographs of the test sites at the NIOSH FSF, depicting the pile of coal rubble, the conveyor haulage frame, conveyor belt, and locations of the gas averaging probe and other detection equipment. The FSF is constructed of masonry block walls, a steel roof, and a concrete floor. The walls and roof are coated with a fire-resistant cementitious coating. The cross-sectional area of the tunnel exit is 11.7 m^2. Air was forced through the gallery using a variable speed axial vane fan at four (4) discrete air velocities—1.0 m/s, 2.0 m/s, 4.0 m/s, and 6.9 m/s. In order to straighten the airflow, ten 0.09 m thick wood panels were placed in front of the fan. The distance from the fan to the middle of the coal bed was 25 m. Tests were conducted using three different types of standard, commonly-used fire resistant conveyor belts, known generically by their primary polymer component as styrene butadiene rubber (SBR), polyvinyl chloride (PVC), and neoprene (NP). Testing all three conveyor belts at each of the four air velocities resulted in a total of twelve (12) experiments.

To ignite the coal, six electrical strip heaters measuring 0.92 × 0.04 m and separated by approximately 0.3 m were imbedded within the pile of coal rubble approximately 5.0 cm below the top surface of the coal (Figure 1b). The strip heaters were rated at 1500 W at 120 V producing a maximum surface temperature of 650°C (1200°F). All heaters were turned off after the coal fire ignited the belt sample and the belt fire was well-developed in the ignition area (typically after 15 min of the belt fire). A 1.8 m wide by 1.5 m long length of belting was placed on the rollers of the conveyer belt structure (21 m long and 1.5 m wide), hanging towards the coal-bed where the strip heaters were fixed. The coal bed consisted of about 350 kg of 1 cm to 5 cm pieces of Pittsburgh coal. The distance from the top surface of the coal pile to the bottom surface of the belt was about 5 cm to 10 cm.

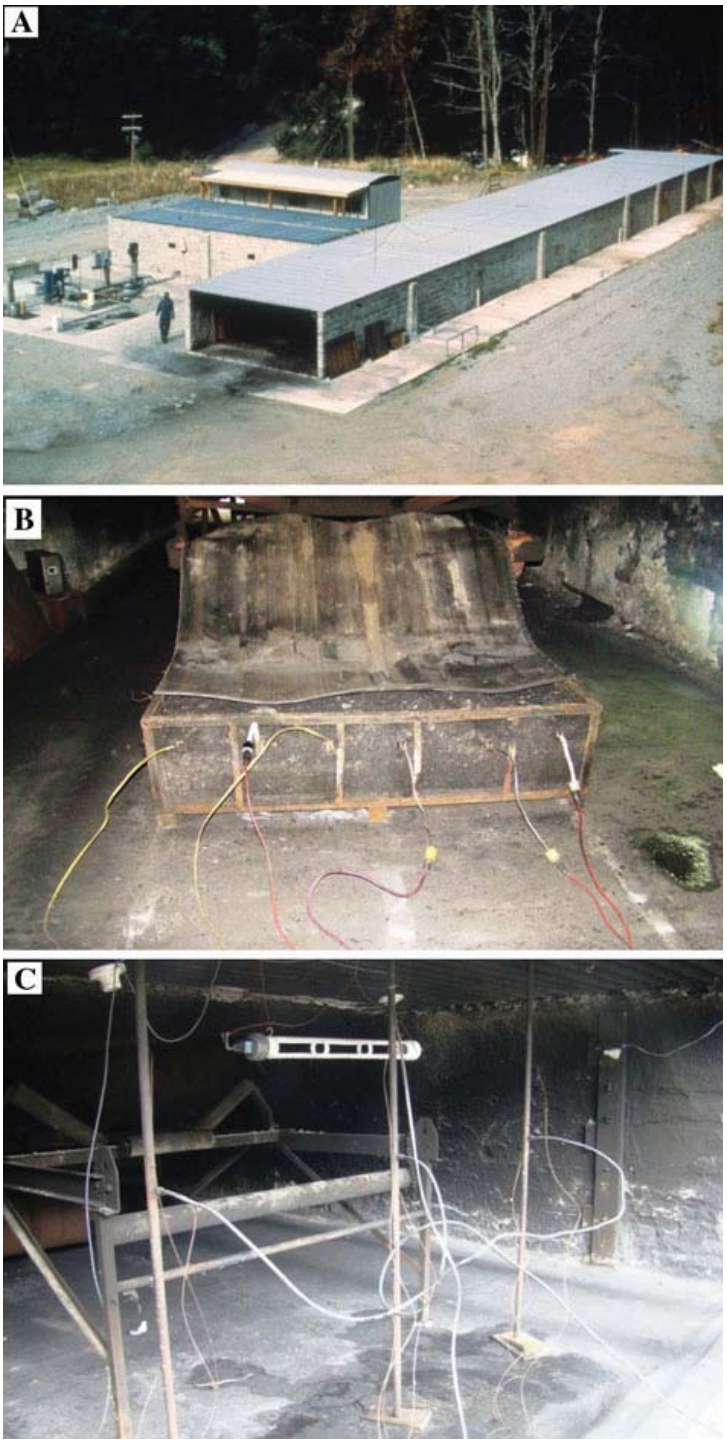

Figure 1. Photographs showing the fire suppression facility (a), the rubblized coal with strip heaters and conveyor belt (b), and the gas sampling and other instrumentation at the exit of the fire suppression facility (c).

The gallery was instrumented with thermocouples to measure the gas temperature. A thermocouple was fixed at the center of the belt to measure the temperature of the fire at the belt ignition (1.5 m from the middle of the coal-bed). Seven thermocouples were connected to the roof from the conveyer belt frame starting at the coal pile, then positioned every 1.5 m to measure the average gas temperature at the exit steam. A smoke and gas sample averaging probe was positioned at the tunnel exit, downstream of the coal pile 19.8 m from the coal bed. This probe was constructed from a 5 cm diameter steel pipe and had four inlet ports spaced at equal intervals along the vertical height of the tunnel to measure the smoke and the gas concentration at the exit stream. The gas samples were analyzed for O_2, CO, and CO_2. An Interscan Corporation RM series Rackmount Monitor[1] CO analyzer with a sensitivity of 0 ppm to 100 ppm was used to measure the CO. An inline filter was used to eliminate interference due to other gases, dust particles, and aerosols. An Infrared Industries IR-208 (see Footnote 1) was used to analyze CO_2 and O_2.

In addition to the gas analysis, two smoke detectors were located near the roof, 19.4 m from the coal pile, to measure the smoke density. The two photoelectric smoke detectors were an ASD FILTREX-F (see Footnote 1) and the diode laser detector PINNACLE (see Footnote 1). Both sensors were fixed to a common fire panel channeled to a computer through an electronic processer. A smoke obscuration meter was also placed 19.4 m downstream from the coal pile, 40 cm from the tunnel roof, to measure the light obscuration at 635 nm. A gas sample was extracted from a point just beyond the obscuration meter and flowed to a TSI DustTrak (see Footnote 1) for simultaneous measurement of smoke mass concentrations. An Axonx (see Footnote 1) video smoke and fire detection system was also used to monitor the visible smoke levels and the progress of the developing fires. Two Axonx video monitors were fixed upstream of the coal fire at 13.4 m and 4.5 m to view the developing fire from two different vantage points.

The outputs of the thermocouples and the analyzers were connected to a 60-channel microprocessor and transmitted to a National Instruments (see Footnote 1) data logger to view the output data. For the initial nine experiments, data were obtained at 10 s intervals and, for the final three experiments, at an air velocity of 6.9 m/s, at 2 s intervals. Experiments were also video recorded.

3. Results and Discussion

3.1. Fire Detection Data and Analysis

Once power was supplied to the electrical strip heaters imbedded within the pile of coal rubble, the mass of coal began to heat, producing smoke for a period of time before finally erupting in flame. Once flaming occurred, the fire intensity increased until the coal flames ignited the conveyor belt material. During these stages of fire growth, the smoke and CO also increased as time progressed. In the 12

[1]Mention of company names or products does not constitute endorsement by the National Institute for Occupational Safety and Health.

experiments conducted, the average time (measured from the moment power was supplied to the electrical strip heaters) to observe the first visible smoke from the smoldering coal was 8 min. From the time the heaters were energized, the average time for the coal to burst into flame was 24 min, or 16 min after smoldering began. These smoldering time periods are comparable to results previously reported [1].

As fire intensity increases, fire hazards also increase, especially subsequent to belt ignition, since it is during this time that rapid flame spread can occur. The primary constraint on the fire detection system is to detect a developing fire prior to belt ignition, or as quickly as possible thereafter before the onset of rapid flame spread can begin [1, 2]. Adopting this constraint, the detection data are best analyzed by comparing the times at which the sensors alarm with the times at which belt ignition occurred. The total time, t_a, needed for a sensor to alarm is the time, t_{conc}, it takes for the fire to produce the required bulk average CO or smoke alarm concentration (as measured from the instant of flaming coal ignition) at a given air velocity plus the travel time, t_t, for this concentration of CO or smoke to travel. On the average, one-half of the distance between two consecutive sensors (150 m or 500 ft) plus the sensor response time, t_r, taken for convenience to be 60 s. For these experiments, the sum of the two latter times, travel time plus sensor response time ($t_t + t_r$) that must be added to the bulk average alarm concentration appearance time, t_{conc}, at the indicated air velocities are:

1. $V_0 = 1.0$ m/s (200 fpm), $t_t + t_r = 210$ s (3.50 min),
2. $V_0 = 2.0$ m/s (400 fpm), $t_t + t_r = 135$ s (2.25 min),
3. $V_0 = 4.1$ m/s (800 fpm) $t_t + t_r = 98$ s (1.63 min), and
4. $V_0 = 6.9$ m/s (1350 fpm) $t_t + t_r = 82$ s (1.37 min).

Figure 2 displays the estimated average times of alarm for a CO sensor at the specified alarm thresholds and spaced at 300 m. The solid curve is the time to belt ignition and represents a value for comparison with the detection times. Points falling above this line represent that the CO detection system failed to detect the developing fire prior to belt ignition, while points falling on or below this line represent that the CO detection system was able to detect the fire just prior to belt ignition. In general, the CO detection appears to satisfy the detection criteria reasonably well (i.e., fire detection must take place before the ignition of the belt). Although there is some scatter in the data with some detection times greater than the time to belt ignition (as should be expected), the overall average was 28.2 s (0.47 min) before belt ignition.

It is also of considerable interest to analyze the data obtained for the smoke sensors. In these experiments it was not possible to measure a bulk average optical density (OD) for the smoke due to both the physical limitations of the gas sample averaging probe and the need to keep the connecting lines of this probe free of contamination. However, estimates of the bulk average OD levels, and thus the times at which the smoke reached the alarm points, can be obtained using previous relationships [1] along with the expressions for the CO and smoke

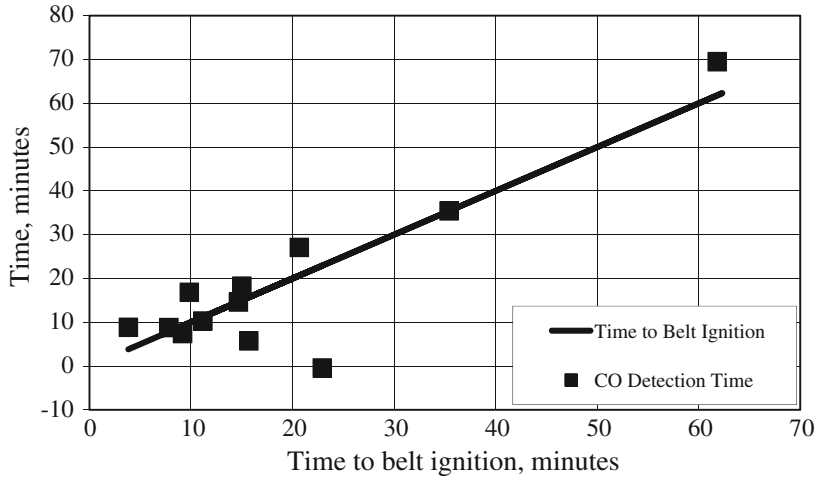

Figure 2. Estimated CO detection times compared to the measured belt ignition times.

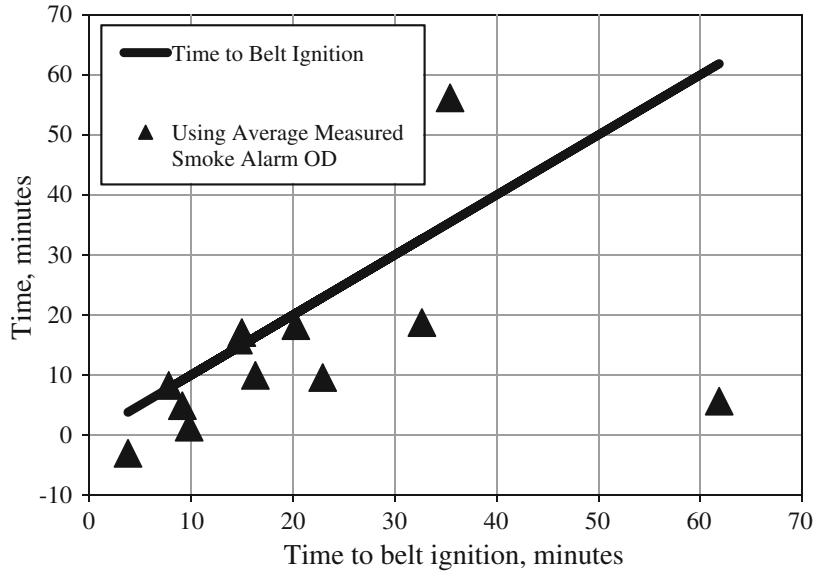

Figure 3. Graph of estimated smoke sensor alarm times relative to the time of belt ignition.

production parameters in Figures 3 and 4 of this report. For CO, the ppm CO is given by the following:

$$\text{ppm CO} = B_{CO} \cdot (Q_F / V_0 A_0) \tag{1}$$

where Q_F = coal fire heat release rate, kW; V_0A_0 = product of ventilation air velocity and entry cross-sectional area, m^3/s; B_{CO} = CO production constant = $4.80 \cdot \exp(-0.175V_0)$; B_{OD} = smoke production constant = $0.037 \cdot \exp(-0.100V_0)$.

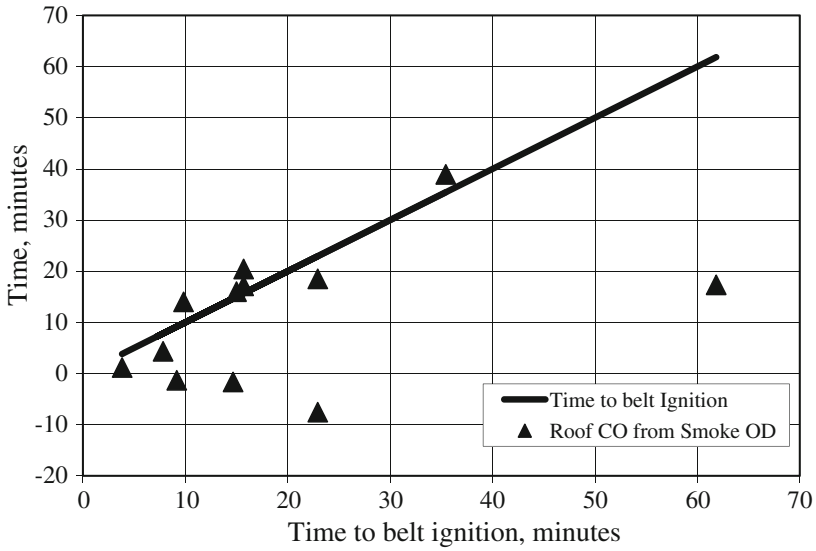

Figure 4. Roof CO alarm times estimated from the smoke optical density.

Similarly, the OD can be calculated using the following:

$$OD = B_{OD} \cdot (Q_F/V_0A_0) \tag{2}$$

The bulk average smoke optical density can be estimated from the measured bulk average CO by combining Equations 1 and 2 and the respective expressions for the CO and smoke production constants, yielding the following:

$$\begin{aligned} OD &= (\text{ppm CO}) \cdot (B_{OD}/B_{CO}) \\ &= (\text{ppm CO}) \cdot 0.00771 \cdot \exp(0.075V_0) \end{aligned} \tag{3}$$

Using this expression, the bulk average smoke OD can be estimated from the measured bulk average CO.

For each experiment, the bulk average smoke OD was plotted as a function of time, and the times to reach the required smoke alarm levels were tabulated as previously done for CO. In addition, the optical density at smoke sensor alarm was measured for the smoke sensors using the smoke obscuration meter located near the roof at the end of the fire tunnel. The average smoke optical density at the moment of smoke sensor alarms was found to be 0.0257 m^{-1}. Table 1 represents the actual OD at the time of smoke sensor alarm and the estimated average time of alarm for CO sensors at the specified alarm thresholds for sensors spaced at 300 m.

Just as in the previous scenario (Figure 2) for CO, the smoke detection system satisfies the detection criteria reasonably well (Figure 3), with results indicating that the smoke sensors typically alarmed before the belt ignited. For the detection times using the measured average OD at alarm of 0.0257 m^{-1}, detection occurred an average of 5.23 min before the belt ignited.

Table 1
CO Detection Times, Smoke Alarm Times, and the Measured Times to Belt Ignition

Test	Air velocity (m/s)	t_{BI} (min)	CO alarm level (ppm)	CO alarm time (min)	Smoke alarm, OD (m^{-1})	Smoke alarm time (min)
SBR	1.0	3.8	9	8.8	0.044	7.5
	2.0	15.0	5	18.3	0.044	18.4
	4.1	7.8	3	8.8	0.022	6.3
	6.9	35.4	1	35.4	0.022	49.8
PVC	1.0	61.8	9	69.5	0.044	25.2
	2.0	9.2	5	7.4	0.044	7.8
	4.1	14.7	3	14.6	0.022	8.8
	6.9	22.9	1	−0.4	0.022	5.4
Neoprene	1.0	9.8	9	16.8	0.044	15.2
	2.0	20.7	5	27.1	0.044	27.4
	4.1	11.2	3	10.3	0.022	9.5
	6.9	15.7	1	5.8	0.022	14.9

The above data and estimates for CO and smoke optical density were for bulk average quantities—the quantities that would exist far downstream of a developing fire after there is essentially complete mixing of the combustion products with the ventilation airflow [8, 9]. Closer to the fire origin, stratification of the combustion products near the roof of an entry occurs, with concentrations decreasing as the distance from the roof increases [8, 9]. In general, the recommendation for product of combustion fire sensors has always been to locate the sensors approximately 0.3 m to 0.5 m below the roof and in the approximate center of the entry in order to take advantage of any possible stratification should the fire occur a short distance upstream of the sensor location.

In keeping with the above sensor location recommendations, two commercially available smoke sensors were located near the end of the tunnel, one on either side of the conveyor belt frame and approximately 0.5 m below the roof of the FSF. A light obscuration meter and the intake port for the smoke mass monitor (DustTrak; see Footnote 1) were also located at the same horizontal and vertical positions, approximately along the centerline of the conveyor belt frame. These locations (satisfying the recommendations noted above) were chosen to obtain additional information on the smoke properties of optical density and mass concentration not only on a continuous basis but, in particular, to measure these quantities at the moment of smoke sensor alarm.

Table 2 shows the alarm times obtained for the smoke sensors and for the Axonx video smoke/flame detection system. Just as for the data on bulk average concentrations presented earlier, all alarm times were measured from the moment of flaming ignition of the coal ($t = 0.0$) so that negative times were best expressed as "minutes before flaming ignition of the coal." On average, the smoke sensors alarmed 4.32 min before flaming coal ignition while the Axonx video smoke system alarmed 9.80 min before flaming coal ignition. It is worth noting that smoke

Table 2
Roof Smoke Sensor, Roof CO, and Video Alarm Times Relative to Flaming Ignition of the Coal

Test	Velocity (m/s)	Roof smoke alarm (min)	Roof CO alarm (min)	Video alarm (min)
SBR	1.0	−16.8	1.7	−15.7
	2.0	−23.8	16	−26.5
	4.1	−12.3	4.3	−16.0
	6.9	NA	38.9	NA
PVC	1.0	NA	17.3	−9.3
	2.0	5.8	−1.3	−20.6
	4.1	−7.7	−1.7	5.3
	6.9	−1.3	−7.6	−3.9
Neoprene	1.0	17.2	14	−8.5
	2.0	−3.3	NA	−18.1
	4.1	2.3	NA	−4.2
	6.9	−3.3	17.1	9.7

sensor alarms were slightly earlier at the higher air velocities (4.1 m/s and 6.9 m/s) than at the lower air velocities (1.0 m/s and 2.0 m/s) (4.44 min and 4.20 min, respectively, before flaming coal ignition). The average earlier detection by the Axonx system may be due either to a higher sensitivity of the equipment or to the location of the video cameras that provided direct viewing of the fire origin.

It is also of interest to estimate the CO concentration near the roof, based on optical density, as the fire develops. Just as the bulk average smoke optical density was estimated based on its relationship to CO in Equations 1–3, the inverse can also be done so that an estimate of the roof CO can be made based upon the measured roof smoke optical density. Solving Equations 1–3 for ppm CO in terms of smoke OD yields the following expression:

$$\text{ppm CO} = \text{OD} \cdot (B_{CO}/B_{OD}) = \text{OD} \cdot 129.73 \cdot \exp(-0.075V_0) \tag{4}$$

Assuming that the smoke and CO stratify in the same manner (a reasonable assumption), then Equation 4 provides a convenient means for estimating the CO concentration near the roof. Using Equation 4, the CO near the roof can be plotted as a function of time using the measured values of smoke optical density. As for the bulk average data, the time at which the alarm concentration is measured (or estimated) is shown in Figure 4. In a manner similar to that observed for the smoke sensor alarms, the estimated alarm times for a CO sensor near the roof often occurred prior to flaming ignition of the coal. On average, the estimated roof CO alarm was activated 8.13 min before the belt ignition. Even accounting for the additional travel time for the bulk average CO, this average roof CO alarm time is significantly more rapid, indicating the advantage of locating sensors near the roof to take advantage of the stratification that may occur at short distances downstream of the fire.

3.2. *Fire Intensities, Growth Rates, and CO Production*

In order to understand the size of the fire at the time of the belt ignition, the heat release rate was calculated using the combustion gases of CO_2 and CO as follows:

$$Q_{TOTAL} = [H_c/k_{CO_2}] \times M_{CO_2} + [(H_c - k_{CO}H_{CO})/k_{CO}] \times M_{CO} \quad (5)$$

where H_c = total (net) heat of combustion of the fuel, kJ/g; H_{CO} = heat of combustion of CO, 10.1 kJ/g; k_{CO_2} = stoichiometric yield of CO_2, g/g ($3.67X_C$, where X_C is the carbon mass fraction); k_{CO} = stoichiometric yield of CO, g/g ($2.33X_C$); M_{CO_2} = generation rate of CO_2 from the fire, g/s (1.97×10^{-3} $V_0A_0\Delta CO_2$); M_{CO} = generation rate of CO from the fire, g/s (1.25×10^{-3} $V_0A_0\Delta CO$); V_0 = air velocity, m/s; A_0 = entry cross-section area, 11.7 m^2; ΔCO_2 = CO_2 produced by fire, ppm; ΔCO = CO produced by fire, ppm.

Substitution of the above parameters for Equation 5 gives

$$Q_{TOTAL} = [1.48 \times 10^{-2}[H_c/k_{CO_2}]\Delta CO_2 + 9.41 \times 10^{-3}[(H_c - k_{CO}H_{CO})/k_{CO}]\Delta CO] \times V_0 \quad (6)$$

The data shown in Table 3 indicate that the ratio of heat release rate to air velocity at belt ignition was found to have an average value of 16.36 kJ/M ± 4.09, which is somewhat lower than previously reported [1]. Because the estimated time for detection of CO (Table 1) occurred after belt ignition in some of the experiments, it is also instructive to calculate this ratio at the time of detection to obtain an estimate of the fire intensity when detection occurs. These ratios are shown in

Table 3
Heat Release Rate and Ratio of Heat Release Rate to Air Velocity at the Time of Belt Ignition, and Ratio of Heat Release Rate to Air Velocity at the Estimated CO Detection Time for the 12 Experiments in this Study

Test	Air velocity (m/s)	Q_F at belt ignition (kW)	Q_F/V_0 at belt ignition	Q_F/V_0 at CO detection
SBR	1.0	16.3	16.0	20.5
	2.0	38.5	18.9	20.5
	4.1	72.2	17.8	22.6
	6.9	100.0	14.6	18.3
PVC	1.0	NA	NA	NA
	2.0	35.7	17.6	15.5
	4.1	45.4	11.2	11.2
	6.9	NA	NA	NA
Neoprene	1.0	19.8	19.5	23.4
	2.0	47.1	23.2	26.2
	4.1	64.8	15.9	16.4
	6.9	61.9	9.0	10.1

column 3 of Table 3, with an average value of 18.46 ± 5.22, indicating that even at the time of detection the fire intensity is relatively lower than expected [1].

In general there is good agreement between the measured and estimated values for CO at belt ignition, especially for experiments conducted at the lower air velocities. For experiments conducted at the higher air velocities, the measured values are, on average, greater than the predicted values by about 2.0 ppm to 2.5 ppm. These higher measured CO values at the higher air velocities would indicate that there may be some flexibility about increasing the CO alarm threshold at the higher air velocities. The average heat release rate, Q_F, and the ratio of heat release rate to ventilation air velocity, (Q_F/V_0), were plotted versus the ventilation air velocity in Figure 5. At higher air velocities the heat release rate increased, but the ratio of heat release rate to ventilation air velocity, Q_F/V_0, was found to be constant. This constant ratio indicates that the resultant CO and smoke levels are not drastically affected when comparing low and high air velocities.

Flame growth rate ($\Delta Q/\Delta t$) was calculated from Equations 5 and 6 using the CO and CO_2 gas concentrations that were measured as a function of time. In these experiments, the flaming coal fire grew at a slower rate than previously reported [1]. The average time for the belt ignition was 16.24 ± 8.32 min. It was found that the fire growth rates increased as the air velocity increased (Figure 6).

Using the CO concentrations and measured heat release rates, the CO production constants were calculated using Equation 1 for different air velocities and are represented in Figure 7. It is interesting to note that the CO production constant as a function of air velocity demonstrates a similar behavior to a previously reported study [1] that also indicated lower CO production at higher velocities.

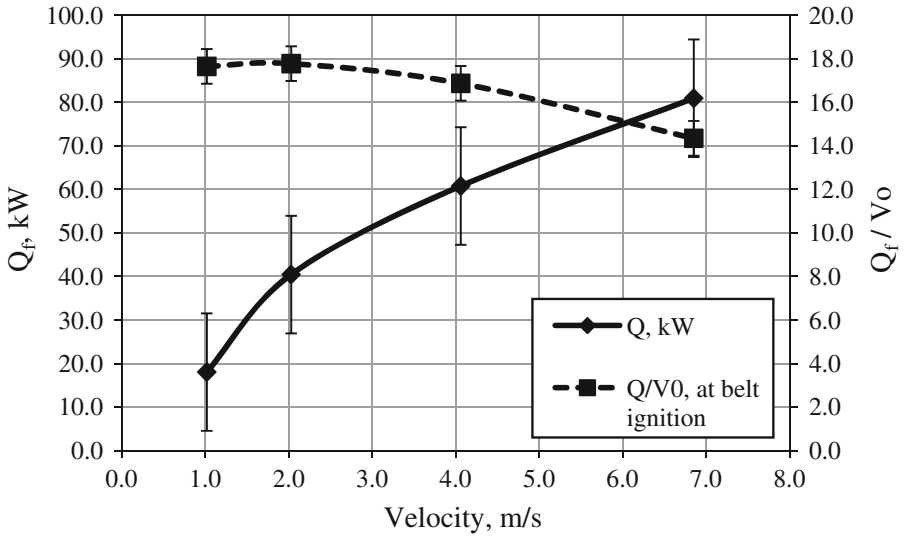

Figure 5. Variation of average heat release (Q_f) and Q_f/V_o at belt ignition.

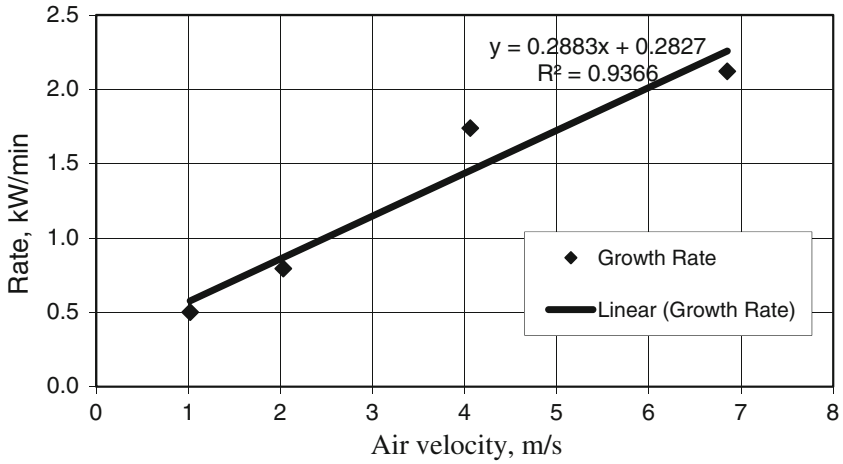

Figure 6. Measured average coal fire growth rates from the time of flaming coal ignition to the time of ignition of the conveyor belts.

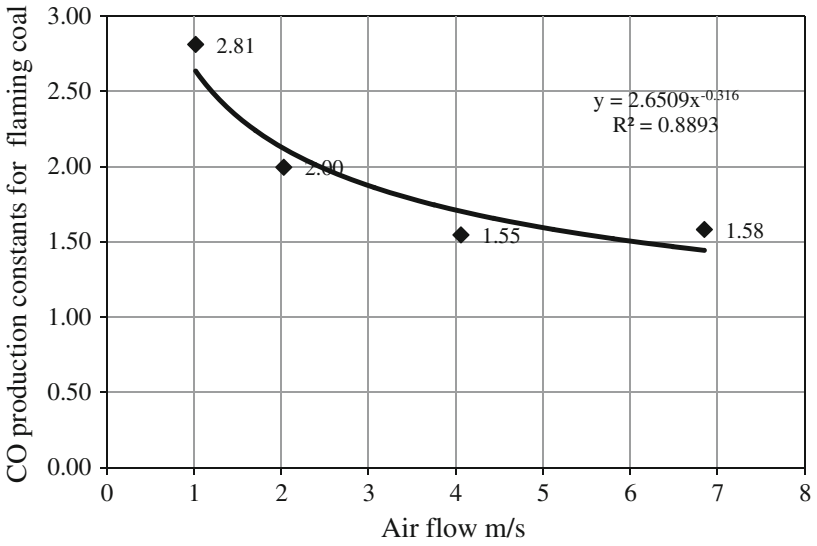

Figure 7. Production constant for CO for flaming coal.

4. Conclusions

Overall the data and analysis presented in this report indicate that ventilation air velocity plays a major role not only in the alarm levels for both CO and smoke optical density but also in the heat release rate and growth rate of conveyor belt fire. In addition, both the air velocity and the cross-sectional area of the fire gallery (11.7 m^2, 126 ft^2) played a role in dictating the alarm levels of the CO and smoke sensors. However, using higher air velocities in entries with smaller cross-sectional areas would tend to increase the alarm levels, meeting the detection criteria as previously reported [1]. For instance, at an air velocity of 4.1 m/s in an entry of 9.29 m^2 (100 ft^2), the indicated alarm level for CO sensors spaced at 304.8-m intervals is 4.0 ppm, and in an entry with a cross-sectional area of

7.43 m^2 (80 ft^2) the indicated CO alarm level would increase to 5.0 ppm. These numbers point to the fact that the sensor alarm levels necessary for adequate fire detection in conveyor belt haulageways will tend to decrease as the air quantity (the product of air velocity and entry cross-sectional area) increases. This would mean that in mines with larger entry cross-sections, greater sensitivity (i.e., lower sensor alarms) would be required than in mines with smaller entry cross-sections, given that the air velocity remains constant—a result primarily of increased dilution of the combustion products by the ventilation airflow.

Disclaimer

The findings and conclusions in this manuscript are those of the authors and do not necessarily represent the views of the national Institute for Occupational Safety and Health (NIOSH). Mention of any company or product does not constitute endorsement by NIOSH.

References

1. Litton CD, Lazzara CP, Perzak FJ (1991) Fire detection for conveyer belt entries. Bureau of Mines Report of Investigations 9380, 23 p
2. Perzak FJ, Litton CD, Mura KE, Lazzara CP (1995) Hazards of conveyor belt fires. Bureau of Mines Report of Investigations 9570, 33 p
3. Litton CD, DeRosa M, Li JS (1987) Calculating fire-throttling of mine ventilation airflow. Bureau of Mines Report of Investigations 9076, 21 p
4. Luzik SJ, Desautels LA (1990) Coal mine fires involving track and belt entries 1970–1988. Bureau of Mines Report of Investigations 09-323-90
5. U.S. Department of Labor (2007) Mine Safety and Health Administration, Report of Investigations 46-08801
6. Title 30—Mineral Resources; Chapter 1—Mine Safety and Health Administration, Department of Labor, Subchapter O—Coal Mine Safety and Health; part 75—Mandatory Safety Standards—Underground Coal Mines (2010)
7. Mutmasky J, Brune J, Calizaya F, Mucho T, Tien J, Weeks J (2007) Final report of the technical study panel on the utilization of belt air and the composition and fire retardant properties of belt in underground coal mining
8. Egan MR (1993) Impact of air velocity on the development and detection of small coal fires. Bureau of Mines Report of Investigations 9480, 15 p
9. Conti RS, Litton CD (1993) Effects of stratification on carbon monoxide levels from mine fires. In: Proceedings of the 6th US mine ventilation symposium, Chap 73